Molecular Pharmacology Fast Forward. Published on September 29, 2014 as DOI: 10.1124/mol.114.094995
This article has not been copyedited and formatted. The final version may differ from this version.

Investigating substrate-induced motion between the scaffold and transport domains in the glutamate transporter EAAT1

Xiuliang Rong, Elia Zomot, Xiuping Zhang and Shaogang Qu

Department of Immunology (S.Q., X.R.)

Department of Biological Chemistry (E.Z.)

Teaching Center of Experimental Medicine (X.Z.)

School of Basic Medical Sciences (S.Q., X.R., X.Z.)

Southern Medical University, Guangzhou, Guangdong 510515, China (S.Q., X.R., X.Z.)

Weizmann Institute of Science, Rehovot, Israel (E.Z.)

Molecular Pharmacology Fast Forward. Published on September 29, 2014 as DOI: 10.1124/mol.114.094995
This article has not been copyedited and formatted. The final version may differ from this version.

Running title: Motion between TM4 and HP1/HP2 in a Glutamate Transporter

correspondence: Shaogang Qu, Ph.D. Department of Immunology, School of Basic Medical Sciences, Southern Medical University, Guangzhou, Guangdong 510515, China. Tel: 86-20-61647275; Fax: 86-20-61648221; E-mail: sgq9528@163.com.

Text pages: 26

Tables: 1

Figures: 6

References: 38

Abstracts: 222 words

Introduction: 741 words

Discussion: 890 words

Abbreviations: EAAT1, Excitatory amino acid transporter 1; HP, Hairpin loop; TM, Transmembrane domain; CuPh, Copper(II) $(1,10\text{-Phenanthroline})_3$; TBOA, D,L-threo-β-benzyloxyaspartate; MTSET, (2-Trimethylammonium)-methanethiosulfonate

Molecular Pharmacology Fast Forward. Published on September 29, 2014 as DOI: 10.1124/mol.114.094995
This article has not been copyedited and formatted. The final version may differ from this version.

Abstract

Excitatory amino acid transporter 1 (EAAT1) plays an important role in keeping the synaptic glutamate concentration below neurotoxic levels by translocating this neurotransmitter into the cell. Both reentrant hairpin loops, HP 1 and 2, have been shown to take part in binding the substrate and the more deeply buried sodium ion, and might therefore be a part of the intra- or extracellular gate of the transporter. However, the shape of the motion of either loop relative to transmembrane domain (TM) 4 during the transport cycle has not yet been fully resolved. Using Copper(II) (1,10-Phenanthroline)$_3$ for crosslinking cysteine pairs, we found strong inhibition of transport when A243C (TM4) was combined with S366C (HP1), I453C (HP2) or T456C (HP2). These findings were reinforced by the impact of cadmium on transport activity, and both approaches consistently showed that proximity was exclusively intra-monomeric. Under conditions that promote the inward-facing state, inhibition by CuPh in A243C/S366C was reduced, while the opposite was seen when the outward-facing one was stabilized suggesting that the two positions are farther apart in the former conformation than in the latter. Surprisingly, maximal crosslinking of A243C with I453C or T456C was not observed under conditions that promote the inward-facing state. Altogether, our data suggest that the transporter may undergo complex relative movement between these positions on TM4 and HP1/HP2 during the transport cycle.

Molecular Pharmacology Fast Forward. Published on September 29, 2014 as DOI: 10.1124/mol.114.094995
This article has not been copyedited and formatted. The final version may differ from this version.

Introduction

Glutamate is the major excitatory neurotransmitter in the mammalian central nervous system (Headley and and Grillner, 1990; Fonnum, 1984). After its release, glutamate is cleared from the synaptic cleft by glutamate transporters (Storck et al., 1992; Tanaka, 1993; Kanner and Sharon, 1978; Zerangue and Kavanaugh, 1996; Levy et al., 1988), which serve to keep its extracellular concentration below neurotoxic levels that can cause cell death following abnormal activation of N-methyl-D-aspartic acid receptors and subsequent calcium entry. These carriers exploit the electrochemical gradient of sodium, generated by the Na^+/K^+-ATPase, in order to drive the energy-consuming intracellular accumulation of glutamate (Kanner and Sharon, 1978; Zerangue and Kavanaugh, 1996; Levy et al., 1988). A typical transport cycle involves the binding of L-glutamate, a proton and three sodium ions to the outward-facing conformation of the transporter after which the transporter shifts to an inward-facing one where the substrates are released to the cytoplasm (Zerangue and Kavanaugh, 1996; Levy et al., 1988). Binding of intracellular potassium follows and the transporter reorients to face the extracellular solvent again where potassium is released before a new cycle can commence (Kanner and Bendahan, 1982; Kavanaugh et al., 1997; Pines and Kanner, 1990). Thus, extracellular sodium with L-glutamate or the replacement of extracellular sodium with potassium increases the proportion of inward-facing transporters. Conversely, external treatment with non-transportable glutamate analogues, such as D, L-threo-β-benzyloxyaspartate (TBOA), locks the transporter in an outward-facing conformation.

The crystal structure of Glt_{Ph}, an archaeal sodium-coupled aspartate symporter from *Pyrococcushorikoshii* that is a homolog of eukaryotic glutamate transporters, has been obtained in outward- and inward-facing conformations, in addition to an intermediate one (Yernool et al., 2004; Boudker et al., 2007; Reyes et al., 2009; Verdon and Boudker, 2012). The obtained crystals show a bowl-shaped homotrimer with a solvent-filled extracellular basin extending halfway across the membrane bilayer (Yernool et al., 2004; Boudker et al., 2007; Reyes et al., 2009). At the bottom of the basin three independent binding sites were observed, one in every subunit, suggesting that the monomer is the functional unit. Support for this idea comes from studies on the glutamate transporter GltT (Goeneveld and Slotboom,

Molecular Pharmacology Fast Forward. Published on September 29, 2014 as DOI: 10.1124/mol.114.094995
This article has not been copyedited and formatted. The final version may differ from this version.

2007) and the excitatory amino acid carrier 1, EAAC1 (Koch and Larsson, 2005; Grewer et al., 2005; Leary et al., 2007; Koch et al., 2007). The monomer includes eight transmembrane (TM) segments, and two reentrant hairpin (HP) loops, the first between TM6 and TM7 (HP1) and the second between TM7 and TM8 (HP2) (Fig. 1A) (Grunewald et al., 1998; Grunewald and Kanner, 2000; Slotboom et al., 1999). The first six transmembrane segments form a distorted 'amino-terminal cylinder' that forms the interface among the subunits, whereas the more conserved TM7 and 8, together with HP1 and 2, form the binding pocket (Yernool et al., 2004). HP1 and HP2 reach from opposite sides of the membrane, and HP2 has been shown to take part in the extracellular gating for the substrate (Yernool et al., 2004; Reyes et al., 2009; Crisman et al., 2009; Huang and Tajkhorshid, 2008; Shrivastava et al., 2008) while HP1 has been hypothesized to be part of the intracellular gate if not the extracellular one as well.

The Glt_{Ph} structures represent static pictures of substrate-occluded conformations of the transporter (Yernool et al., 2004; Boudker et al., 2007; Reyes et al., 2009; Verdon and Boudker, 2012). During the complete transport cycle, however, many other conformations are visited as well. A major difference between the outward- and inward-facing conformations is the translation of the binding pocket by ~ 15Å and rotation by ~ 30° relative to the rest of the protein from the extracellular to the intracellular side (Reyes et al., 2009; Verdon and Boudker, 2012). However, many of the details of the conformational changes associated with the transport cycle are not yet clear. In order to analyze the spatial proximity between TM4/HP1 and TM4/HP2 in the human excitatory amino acid transporter 1 (EAAT1), we used as reference the crystallized outward- and inward-facing forms of Glt_{Ph} ((Yernool et al., 2004; Boudker et al., 2007; Reyes et al., 2009) (Fig. 1).We explore here the aqueous accessibility and potential spatial proximity between cysteines pairs introduced into TM4 and HP1 (Fig. 1A) as well as into TM4 and HP2 (Fig. 1B) guided by the outward- and inward-facing structures of Glt_{Ph}, respectively. In both cases, our findings strongly support that spatial proximity is altered during the transport cycle and that the motion of the transport core is more complex and dynamic than formerly proposed.

Molecular Pharmacology Fast Forward. Published on September 29, 2014 as DOI: 10.1124/mol.114.094995
This article has not been copyedited and formatted. The final version may differ from this version.

MATERIALS AND METHODS

Generation and Subcloning of Mutants

Site-directed mutants were generated in EAAT1 construct using the method by Kunkel et al. (Kunkel et al., 1987; Kleinberger-Doron and Kanner, 1994) using a uracil-containing single-stranded wild-type or cysteine-less EAAT1 DNA (ssU-DNA) as a template. After transformation of the *E. coli* dut^- ung^- strain with the wild-type DNA, the sense strand of this uracil-containing DNA is produced using a phage that recognizes the f1 origin of the pBS vector. Mutagenic primers were designed as antisense and annealed to this ssU-DNA and the complementary strand synthesized. Restriction enzymes *BsrG*I and *BstE*II or *BstE*II and *Sac*I were used to subclone the mutations into the construct containing EAAT1 in the pBluescript SK(–) vector (Stratagene). The subcloned DNA fragments were sequenced in both directions between the two noted restriction sites.

Cell Growth and Expression

HeLa cells (purchased from ATCC, Manassas, VA) were cultured in Dulbecco's modified Eagle's medium (DMEM) supplemented with 10% fetal calf serum (FCS), 200 units/ml penicillin, 200 µg/ml streptomycin, and 2 mM glutamine. Heterologous expression of the wild type and mutant transporters was done as follows: Confluent HeLa cell culture was split 1:8 with fresh medium and plated into 24-well plates. After 16-22 hours, HeLa cells were infected with recombinant vaccinia/T7 virus vTF (Fuerst et al., 1986) by application of 150µl of the virus/DMEM mix (lacking FCS) and incubation at 37^{o}C for approximately 30 min prior to transfection with DNA (pBluescript SK with the wild type or mutant transporter inserted downstream to the T7 promoter) using the transfection reagent DOTAP. Transfection was carried out by applying 200 µl of the DNA/DOTAP/DMEM mix (lacking FCS) as described (Keynan et al., 1992).

Transport

Transport of radioactive D-[^{3}H]-aspartate was measured 16-20 hours post transfection and incubation at 37^{o}C. The wells were washed once with 1 ml of ChCl solution (150 mM choline chloride, 5 mM KP_i, pH 7.4, 0.5 mM $MgSO_4$, and 0.3 mM $CaCl_2$). Each well was then incubated with 200 µl NaCl solution (150 mM NaCl, 5 mM KP_i, pH 7.4, 0.5 mM $MgSO_4$, and

Molecular Pharmacology Fast Forward. Published on September 29, 2014 as DOI: 10.1124/mol.114.094995
This article has not been copyedited and formatted. The final version may differ from this version.

0.3 mM $CaCl_2$) supplemented with 0.4 µCi of the D-[^{3}H]-aspartate and incubated for 10 min at room temperature. Uptake was stopped after 10 min by removing the transport medium and washing the cells twice with cold sodium solution. Cells were lysed in 1% SDS and the radiolabel accumulated in the cells was measured by liquid scintillation counting.

Inhibition of Transport by CuPh

HeLa cells transfected with the indicated constructs were washed once with choline solution and preincubated for 5 min in the presence and absence of CuPh. The preincubation solution contained the indicated concentrations of CuPh (see the figure legends). The indicated preincubation solutions contained NaCl, NaCl + 1 mM L-glutamate, choline chloride (ChCl) + 1 mM L-glutamate, NaCl + 1 mM GABA, NaCl + 20 µM TBOA, ChCl + 20 µM TBOA, KCl (150 mM KCl, 5 mM KP_i, pH 7.4, 0.5 mM $MgSO_4$, and 0.3 mM $CaCl_2$) or ChCl respectively in the different experiments. After 5 min, the medium was aspirated, and the cells were washed twice with 1 ml of the choline solution followed by the transport assay using 200 µl transport medium supplemented with 0.4 µCi of the tritium-labeled substrate for each well. Each experiment was performed at least three times. The optimal concentration of CuPh for the double mutants, indicated in the figure legends, was determined by preliminary titration experiments. The CuPh stock solution was prepared for each experiment by mixing 0.4 ml of 1.25 M 1,10-phenanthrolinein water:ethanol (1:1) and 0.6 ml of 250 mM $CuSO_4$.

Kinetics

HeLa cells were plated into 24-well plate. After 16-22 hours, HeLa cells were infected with recombinant vaccinia/T7 virus vTF. HeLa cells incubation at 37 ^oC for 30 min, followed by transfected with DNA by using transfection reagent DOTAP. After 16-20 hours transfection, HeLa cells expressing EAAT1, CL-EAAT1 or cysteine substitution mutants were incubated with or without CuPh for 5 min at room temperature. Subsequently, cells were washed twice with choline solution. Then substrate transport was carried out with 154 nM D-[^{3}H]-aspartate in final unlabled D-Aspartate concentrations of 1, 3, 10, 50, 100, 300, 500, 1000 µM for 10 min at room temperature. K_m and V_{max} values got from the Hill equation by using the non-linear fitting in the Origin 7.5 software (Origin 7.5 software, Northampton, MA, USA).

Molecular Pharmacology Fast Forward. Published on September 29, 2014 as DOI: 10.1124/mol.114.094995
This article has not been copyedited and formatted. The final version may differ from this version.

The V_{max} is expressed as a percent of that of EAAT1 or CL-EAAT1 without CuPh treatment.

Inhibition Studies with Sulfhydryl Reagents

Before the transport measurements, the cells adhering to 24-well plates were washed with the choline solution and incubated with 200 µl of the indicated solution containing MTSET [(2-trimethylammonium) methanethiosulfonate] for 5 min. The indicated solutions contained NaCl, NaCl + 1 mM L-glutamate, NaCl + 20 µM TBOA, KCl or ChCl. The cells were then washed twice with 1 ml of choline solution before the 10 min uptake assay was initiated by adding 200 µl of the sodium solution with D-[^{3}H]-aspartate at room temperature. Each experiment was performed at least three times in triplicates. The concentration of MTSET was optimized for each mutant as indicated in the figure legends.

Restoration of Activity by DTT

HeLa cells expressing EAAT1 or double mutant were preincubated with CuPh for 5 min at room temperature, washed twice with choline chloride-containing solution, and preincubated with 20 mM dithiothreitol (DTT) for 5 min at room temperature, washed again and subsequently the uptake activity was measured.

Inhibition of Transport by Cd^{2+}

HeLa cells transfected with the indicated construct were washed once with choline solution and preincubated with 500 µM cadmium chloride in transport solution (150 mM NaCl, 5 mM KPi pH 7.4, 0.5 mM MgSO4, and 0.3 mM $CaCl_2$) with the tritium-labeled substrate for 10 min at room temperature. Uptake was terminated after 10 min by removing the transport solution and washing the cells twice with cold sodium solution. HeLa cells were lyzed with SDS followed by scintillation counting.

Statistical analysis

All the data were presented as means ± standard error from three independent experiments. One-way ANOVA with post-hoc multiple comparison or Student's *t* test were used to accomplish the statistical analyses with the SPSS 16.0 statistical software. Differences were

Molecular Pharmacology Fast Forward. Published on September 29, 2014 as DOI: 10.1124/mol.114.094995
This article has not been copyedited and formatted. The final version may differ from this version.

considered significant at $P < 0.05$ or $P < 0.01$.

Molecular Pharmacology Fast Forward. Published on September 29, 2014 as DOI: 10.1124/mol.114.094995
This article has not been copyedited and formatted. The final version may differ from this version.

RESULTS

Inhibition of activity in A243C/S366C by thiol cross-linking and cadmium coordination

The outward-facing structure of Glt_{Ph} suggests that Val151 located on TM4 and Ser279 at the tip of HP1 may be close to each other (Boudker et al., 2007). We have therefore simultaneously replaced the equivalents of these positions in EAAT1, Ala243 (on TM4) and Ser366 (on HP1) with cysteines. This was initially performed in the background of the cysteine-less (CL) version of EAAT1 which contains the C186S, C252A and C375G substitutions and has ~ 70% of the activity of wild type-EAAT1. Transport activity of the A243C/S366C double mutant was too low to allow meaningful further investigation (4.6 ± 0.7% of that of CL-EAAT1, n = 3) and so the A243C/S366C double mutant was introduced into the wild type (WT) EAAT1 where it exhibited higher activity (15.6 ± 1.1% of that of WT, n = 3) while that of the single mutants A243C and S366C was 37.4 ± 2.3 and 46.8 ± 3.5%, respectively.

Transport activity in A243C/S366C-EAAT1 expressed in HeLa cells, assayed using radiolabeled D-aspartate, was measured with or without pretreatment with the thiol-crosslinking reagent Copper(II)(1,10-Phenanthroline)$_3$ (CuPh). In contrast to the WT, where little or no effect was seen as 92.1 ± 4.5% of activity was retained with up to 800 µM CuPh (Fig. 2A), A243C/S366C exhibited a dramatic decrease in transport activity following exposure to the crosslinking reagent in a dose-dependent manner; 50% inhibition was observed at 200 µM while transport activity was almost abolished at 800 µM CuPh (Fig. 2A). This effect could be caused by the two introduced cysteines forming a disulfide bond with each other or with other endogenous cysteines (Brocke et al., 2002; Zomot et al., 2005; Leighton et al., 2006), which could restrict the protein motion during the transport cycle.

In contrast to the double cysteine mutant, inhibition by CuPh was not seen in cells expressing either WT-EAAT1 or the single cysteine replacements A243C or S366C (Fig. 2B). This rules out the involvement of other endogenous cysteines in the observed effect of CuPh and validates the use of WT background to further probe proximity between positions 243 and 366. In addition, inhibition by CuPh was only observed when the cysteines at both sites were present on the same subunit, but not when they resided on different ones as demonstrated by

Molecular Pharmacology Fast Forward. Published on September 29, 2014 as DOI: 10.1124/mol.114.094995
This article has not been copyedited and formatted. The final version may differ from this version.

the lack of inhibition in cells cotransfected with the single cysteine mutants (Fig. 2B). This suggests that the cysteines at positions 243 and 366 come into proximity within the monomeric unit, but not at the interface between the monomers. Moreover, no effect of CuPh was seen upon introducing non-cysteine residues at either site, such as in A243C/S366A or A243S/S366C (Fig. 2B), indicating the unlikelihood of either position to form a disulfide bond with an endogenous cysteine upon perturbing the other site. To measure the influence of cross-linking on the kinetic parameters of the mutants, we detected the maximum transport rate (V_{max}) and the apparent transport affinity (K_m) of D-Aspartate with or without CuPh. As shown in the table 1, the A243C/S366C mutant exhibited a lower V_{max} after exposure to CuPh. In rare instances, CuPh may lead to the formation of a covalent bond between a sulfhydryl and another chemical group. We have therefore also used the reducing agent dithiothreitol (DTT) in order to rule out this unlikely possibility. Following treatment with 20mM DTT, 82.5 ± 3.7% (n=3) of activity was restored in A243C/S366C. Upon comparison with the WT, where 92.1 ± 4.5% of uptake was retained, this is an almost full effect by DTT and further evidence to the formation of a CuPh-induced disulfide bond between the two introduced cysteines.

Although the strongest inhibitory effect of CuPh was observed in the A243C/S366C, we looked for additional evidence that these two positions could be close in space and examined the ability of the double cysteine mutant to form a high affinity metal binding site, such as that of cadmium (Cd^{2+}). This divalent cation can interact with a cysteinyl side chain (Perez-Garcia et al., 1996) and the affinity of the interaction is dramatically increased if it is coordinated by two such groups (Benitah et al., 1996). Exposure of the A243C and S366C single mutants to up to 500 μM Cd^{2+} had very little effect on D-[^{3}H]-aspartate uptake, and the same is true for the A243C/S366A and A243S/S366C double mutants (Fig. 3). However, in contrast to these controls, inhibition of ~76% was observed on uptake by A243C/S366C by Cd^{2+} (Fig. 3) and this inhibition was only present when the cysteine pair was introduced in the same polypeptide and not when the single cysteine mutants were coexpressed (Fig. 3), strongly supporting that the two positions come in proximity in the same and not different monomeric units. Our results of both disulfide bond formation and Cd^{2+}-coordination thus far show that Ala-243 in TM4 is indeed in intramolecular spatial proximity to Ser-366 in HP1.

Molecular Pharmacology Fast Forward. Published on September 29, 2014 as DOI: 10.1124/mol.114.094995
This article has not been copyedited and formatted. The final version may differ from this version.

Effect of glutamate and TBOA on cross-linking in A243C/S366C

To determine the effect of the composition of the external solution on the oxidative inhibitory effect, the A243C/S366C double mutant was incubated for 5 min with 200 μM CuPh, a concentration at which approximately half-maximal inhibition was observed in NaCl, under various external conditions. When external sodium was either supplemented with glutamate or replaced by potassium, conditions that promote the formation of the inward-facing conformation (Reyes et al., 2009; Shlaifer and Kanner, 2007), a reduction in the degree of inhibition by CuPh was observed (Fig. 4A), suggesting that the two introduced cysteines either move farther apart or become obscured from each other in an intermediate or inward-facing conformation. The protection by L-glutamate was not seen in the absence of sodium (choline replacement; Fig. 4A) or with γ-aminobutyric acid (GABA), which is not a substrate of EAAT1 (Fig. 4A). Also, effect by glutamate required the presence of sodium indicating that the former is unable to independently induce the protective conformational change. In contrast, the non-transportable substrate analogue TBOA, which is expected to increase the proportion of outward-facing transporters (Boudker et al., 2007), potentiated the effect of CuPh (Fig. 4A). This effect of TBOA was not due to incomplete removal of the antagonist as WT and A243C/S366C treated only with TBOA in our experiments retained 92±3.5% and 93±4.2% of activity, respectively, compared with the untreated samples.

Aqueous accessibility of cysteines introduced at positions 243 and 366

In addition to the distance between the two sulfhydryl groups, the aqueous accessibility thereof can also impact the degree of inhibition by Cd^{2+} or CuPh. Therefore, we explored the effect of reagents that specifically react with aqueously-exposed sulfhydryl groups on transport to explore the accessibility of each site in CL-EAAT1, where the respective activity of A243C and S366C is 19.2 ± 1.8% and 40.1 ± 2.4% of that of CL-EAAT1. Preincubation of A243C with the membrane-impermeable sulfhydryl-reactive MTSET resulted in ~ 35% inhibition of transport when sodium was present (Fig. 4B). Addition of L-glutamate or replacement of external sodium with potassium, each of which protected against CuPh did not have an effect on the inhibition of A243C by MTSET. However, a moderate (~ 15%) increase

Molecular Pharmacology Fast Forward. Published on September 29, 2014 as DOI: 10.1124/mol.114.094995
This article has not been copyedited and formatted. The final version may differ from this version.

in inhibition was seen in the presence of TBOA (Fig. 4B). Previously, the cysteine at position 366 was seen to be more variably inhibited by MTSET under different external conditions; potassium or L-glutamate with sodium were able to protect against inhibition (by ~ 25%) while TBOA had no effect (Zhang et al., 2014). In both mutants, however, little or no effect was seen upon removal of external sodium (replacement with choline) (Fig. 4B) (Zhang et al., 2014). In contrast to the single cysteine mutants, no significant inhibition by MTSET was observed in CL-EAAT1 under all tested conditions (remaining activity 94 - 96%) and the same is true for the control mutants A243S and S366A (data not shown).

Crosslinking of cysteine pairs introduced into TM4 and HP2 complement those of A243C/S366C

In order to gain a deeper understanding of the population of the global outward- and inward-facing states of EAAT1, we have also explored potential proximity between sites on TM4 and HP2 in the inward-facing conformation of EAAT1 according to the relevant resolved structure of Glt_{Ph} (Reyes et al., 2009). To this aim, we selected two positions on HP2, Ile453 and Thr456 that can potentially move towards Ala243 during the transport cycle. This selection was based on the Glt_{Ph} equivalents of these sites, Met365 and Glu368 (HP2), which may be close to Val151 on TM4, with a Cβ-Cβ distance of less than 6Å in each case (Fig. 1B). The double-mutants each had a respective activity of 59.6 ± 4.3% and 21.6 ± 2.7% of that of CL-EAAT1 (n = 3). Therein, A243C/I453C as well as A243C/T456C displayed strong dose-dependent inhibition of activity in response to CuPh, and this response was observed only when both cysteines, and not either, were engineered into CL-EAAT1 (Fig. 5A, B, C) and only when they were introduced into the same monomeric unit but not when HeLa cells were simultaneously transfected with the two single-cysteine constructs (Fig. 5B, C). As shown in the table 1, the A243C/I453C mutant showed a remarkably lower transport affinity after incubation with CuPh while the two double mutants exhibited a lower V_{max} after exposure to CuPh. From the assay of transport kinetics, we found that the disulfide bond formation between TM4 and HP1 or HP2 damaged transport function. Moreover, the disulfide bond formation between A243C and I453C also weakened its ability of binding substrate. As previously seen in A243C/S366C, following treatment with CuPh (15 μM), DTT

Molecular Pharmacology Fast Forward. Published on September 29, 2014 as DOI: 10.1124/mol.114.094995
This article has not been copyedited and formatted. The final version may differ from this version.

(20 mM) was able to restore activity almost completely in A243C/I453C and A243C/T456C (CL background) with respective values of 87.1 ± 5.6% and 92.0 ± 3.1%, compared to 95.3 ± 5.2% in CL-EAAT1(n=3).

In further support of the spatial proximity of these two sites, external Cd^{2+} was able to abolish almost completely any activity in each double cysteine mutant (Fig. 5D, E). Consistently, this effect took place only in the double, but not single, cysteine mutants and only when each of the cysteine pairs, A243C/I453C or A243C/T456C, was engineered into the same monomeric unit (Fig. 5D, E). Interestingly though, the degree of inhibition by CuPh in A243C/T456C cannot be interpreted merely in terms of the global state of the transporter, inward- or outward-facing, as previously with A243C/S366C. This is because both external conditions that promote (potassium or sodium with L-glutamate) or reduce (TBOA with sodium) the inward-facing population of the transporter protected against crosslinking in comparison to sodium only (Fig. 6B). Also here, we probed the effect of MTSET on each single-cysteine mutant in the CL-EAAT1 background and found that both positions are externally accessible with 50% or 70% activity remaining at 0.05 or 2 mM MTSET in I453C or T456C, respectively (Fig. 6C, D). However, while adding glutamate to sodium moderately protected against inhibition by MTSET in T456C, potassium moderately protected against inhibition in the case of T456C while surprisingly increased that in I453C (Fig. 6C, D).

Molecular Pharmacology Fast Forward. Published on September 29, 2014 as DOI: 10.1124/mol.114.094995
This article has not been copyedited and formatted. The final version may differ from this version.

DISCUSSION

Prior to the determination of the crystal structure of the aspartate symporters Glt_{Ph}, experimental work had shown that in GLT-1 a cysteine replacing Ala364 in HP1, which corresponds to Ser366 of EAAT1, can be close in space to another inserted at Ser440 located at the tip of the HP2 (Brocke et al., 2002) and that the tip of HP1 is also close to the middle of TM7 (Leighton et al., 2006). While such studies were performed on pairs of cysteines within the 'transport core' of glutamate transporters, here we investigated spatial proximity of the tip of HP1 to TM4, which is part of the 'scaffold' domain that largely provides the interface between the monomeric units and support for the transport core. The latter domain can shift between the outer- and inner-facing states, each of which can include several substates, with additional states and/or substates visited along this pathway such as the crystallized intermediate conformation (Verdon and Boudker, 2012). The equilibrium between these conformations is shifted based on the composition of the external and internal solvents that determine the electrochemical gradient of the substrate and its analogues and the co- and counter-translated ions. The crystal structure of the homologous aspartate symporter Glt_{Ph} shows that the α-carbon atoms of the two positions equivalent to Ala243 and Ser366 in EAAT1 are separated by ~7Å in an outward- and ~24Å in an inward-facing conformation (Fig. 1) and this shift is supported by an experimentally validated model thereof (Crisman et al., 2009). This difference is caused mostly by the translation and rotation of the transport core, on which Ser-366 is located, into the cytoplasm relative to the scaffold where Ala-243 is located. Whereas in the outward-facing conformation Ser-366 is accessible to the external medium and in the inward-facing one to the cytoplasm, the accessibility of Ala-243 to the external solvent in both cases is similar. Therefore, by stabilizing the conformation in which the two cysteines are close, TBOA increases inhibition by crosslinking. In contrast, the substrate, which induces the whole transport cycle causes the transporter to reside in the inward-facing state as well, decreases the observed inhibition and the same is true for external potassium.

The accessibility of the cysteine inserted at either position to the externally-applied MTSET indicates that the increase or decrease in crosslinking by CuPh is a result of the motion of the

Molecular Pharmacology Fast Forward. Published on September 29, 2014 as DOI: 10.1124/mol.114.094995
This article has not been copyedited and formatted. The final version may differ from this version.

transport core relative to the scaffold and not due to merely obscuring either cysteine from the other by structural rearrangements. This is supported by the observation that A243C is accessible to MTSET in a manner not affected by the composition of the external medium in contrast to S366C that is inhibited to different degrees by MTSET. Thus, while Ala-243 on the scaffold remains externally accessible, Ser-366 on the transport core shifts between both sides of the membrane. Even under conditions that promote the conformational transition of the transport core to the cytoplasm, such as the addition of the substrate or replacement of sodium by potassium, protection cannot be complete since the inward-facing conformation can still bind intracellular sodium and glutamate (or aspartate) and reorient to face the extracellular side again.

Further support for this transition comes not only from the crystal structures of the outward- and inward-facing conformations but also from studies showing that while parts of the transport core are mobile, the scaffold is largely not. For instance, the equivalent of Ser-366 in the prokaryotic Glt_{Bs}, Glu-271, was shown to be accessible from both sides of the membrane using maleimide labeling (22). In addition, because the trimeric interface has been shown in the bacterial glutamate transporter GltT to be unchanged during transport when cysteines introduced into TMs 2, 4 and 5 were crosslinked (Goeneveld and Slotboom, 2007), this conformational change will likely involve HP1 in EAAT1 as well. Recent insight on the dynamics of Glt_{Ph} using single molecule FRET (smFRET) has shown that the inward-facing state favors the binding of Na^+ or Na^+/Asp^- (Akyuz et al., 2013). We observe here that in EAAT1 not only the Na^+/Glu^-- but also the Na^+-bound and apo transport core can undergo significant inward motion relative to the scaffold. This is evident based on the proximity between each of Ile453 and Thr456, both located on the extracellular side of HP2, and Ala243 on TM4. However, the fact that the substrate protects against this crosslinking in A243C/T456C, provided sodium is present, indicates that the overall motion may be different from a simple straight one that connects the two crystallized conformations (Fig. 1) or that the transport core can move more inwards than observed in the crystallized inward-facing form. It is also possible that the two domains, although close in the inward-facing state, may become shielded from each other or that when the substrate is bound. While TBOA in the presence of sodium moderately protected T456C in HP2 against crosslinking with A243C on TM4, it is

Molecular Pharmacology Fast Forward. Published on September 29, 2014 as DOI: 10.1124/mol.114.094995
This article has not been copyedited and formatted. The final version may differ from this version.

unclear whether this effect is due to stabilizing EAAT1 in an outward-facing conformation or due to interference by EL3-4. Further work is required to address this issue as binding of TBOA could shield HP2 from the external solution, as supported both by the varying external accessibility of both positions (results with MSTET) and by the observation that EL3-4 in the homologous Glt_{Ph} undergoes conformational changes upon binding aspartate or TBOA in the presence of sodium (Compton et al., 2010).

Molecular Pharmacology Fast Forward. Published on September 29, 2014 as DOI: 10.1124/mol.114.094995
This article has not been copyedited and formatted. The final version may differ from this version.

AUTHORSHIP CONTRIBUTIONS

Participated in research design: Qu

Conducted experiments: Rong, Zomot and Zhang

Performed data analysis: Qu, Rong and Zomot

Wrote or contributed to the writing of the manuscript: Qu, Zomot and Rong

Molecular Pharmacology Fast Forward. Published on September 29, 2014 as DOI: 10.1124/mol.114.094995
This article has not been copyedited and formatted. The final version may differ from this version.

REFERENCES

Akyuz N, Altman RB, Blanchard SC, Boudker O (2013) Transport dynamics in a glutamate transporter homologue. *Nature* **502:**114-118

Benitah JP, Tomaselli GF, Marban E (1996) Adjacent pore-lining residues within sodium channels identified by paired cysteine mutagenesis. *Proc Natl Acad Sci U S A* **93:**7392-7396

Boudker O, Ryan RM, Yernool D, Shimamoto K, Gouaux E (2007) Coupling substrate and ion binding to extracellular gate of a sodium-dependent aspartate transporter. *Nature* **445:** 387-393

Brocke L, Bendahan A, Grunewald M, Kanner BI (2002) Proximity of two oppositely oriented reentrant loops in the glutamate transporter GLT-1 identified by paired cysteine mutagenesis. *J. Biol. Chem.* **277:** 3985-3992

Compton EL, Taylor EM, Mindell JA (2010) The 3-4 loop of an archaeal glutamate transporter homolog experiences ligand-induced structural changes and is essential for transport. *Proc Natl Acad Sci U S A* **107:**12840-12845

Crisman TJ, Qu S, Kanner BI, Forrest LR (2009) Inward-facing conformation of glutamate transporters as revealed by their inverted-topology structural repeats. *Proc Natl Acad Sci U S A* **10:**20752-20757

Fonnum F (1984) Glutamate: a neurotransmitter in mammalian brain. *J Neurochem* **42:**1-11

Fuerst TR, Niles EG, Studier FW, Moss B (1986) Eukaryotic transient-expression system based on recombinant vaccinia virus that synthesizes bacteriophage T7 RNA polymerase. *Proc Natl Acad Sci U S A* **83:**8122-8126

Goeneveld M, Slotboom DJ (2007) Rigidity of the subunit interfaces of the trimeric glutamate transporter GltT during translocation. *J Mol Bio* **372**:565-570

Grewer C, Balani P, Weidenfeller C, Bartusel T, Tao Z, Rauen T (2005) Individual subunits of the glutamate transporter EAAC1 homotrimer function independently of each other. *Biochemistry* **44:**11913-11923

Grunewald M, Bendahan A, Kanner BI (1998) Biotinylation of single cysteine mutants of the glutamate transporter GLT-1 from rat brain reveals its unusual topology. *Neuron* **21:**623-632

Grunewald M, Kanner BI (2000) The accessibility of a novel reentrant loop of the glutamate transporter GLT-1 is restricted by its substrate. *J Biol Chem* **275:**9684-9689

Headley PM, Grillner S (1990) Excitatory amino acids and synaptic transmission: the evidence for a physiological function. *Trends Pharmacol Sci* **11:**205-211

Huang Z, Tajkhorshid E (2008) Dynamics of the extracellular gate and ion-substrate coupling in the glutamate transporter. *Biophys J* **95:**2292-2300

Kanner BI, Sharon I (1978) Active transport of L-glutamate by membrane vesicles isolated from rat brain.*Biochemistry* **17:**3949-3953

Kanner BI, Bendahan A (1982) Binding order of substrates to the sodium and potassium ion coupled L-glutamic acid transporter from rat brain. *Biochemistry* **21:**6327-6330

Kavanaugh MP, Bendahan A, Zerangue N, Zhang Y, Kanner BI (1997) Mutation of an amino acid residue influencing potassium coupling in the glutamate transporter GLT-1 induces obligate exchange. *J Biol Chem* **272:**1703-1708

Keynan S, Suh YJ, Kanner BI, Rudnick G (1992) Expression of a cloned gamma-aminobutyric acid transporter in mammalian cells. *Biochemistry* **31:** 1974-1979

Kleinberger-Doron N, Kanner BI (1994) Identification of tryptophan residues critical for the function and targeting of the gamma-aminobutyric acid transporter (subtype A). *J Biol Chem* **269:**3063-3067

Koch HP, Larsson HP (2005) Small-scale molecular motions accomplish glutamate uptake in human glutamate transporters. *J Neurosci* **25:**1730-1736

Koch HP, Brown RL, Larsson HP (2007) The glutamate-activated anion conductance in excitatory amino acid transporters is gated independently by the individual subunits. *J Neurosci* **27:**2943-2947

Kunkel TA, Roberts JD, Zakour RA (1987) Rapid and efficient site-specific mutagenesis without phenotypic selection. *Methods. Enzymol* **154:**367-382

Leary GP, Stone EF, Holley DC, Kavanaugh MP (2007) The glutamate and chloride permeation pathways are colocalized in individual neuronal glutamate transporter subunits. *J Neurosci* **27:**2938-2942

Leighton BH, Seal RP, Watts SD, Skyba MO, Amara SG (2006) Structural rearrangements at the translocation pore of the human glutamate transporter, EAAT1. *J Biol Chem* **281:**29788-29796

Levy LM, Warr O, Attwell D (1988) Stoichiometry of the glial glutamate transporter GLT-1 expressed inducibly in a Chinese hamster ovary cell line selected for low endogenous Na^+-dependent glutamate uptake. *J Neurosci* **18:**9620-9628

Perez-Garcia MT, Chiamvimonvat N, Marban E, Tomaselli GF (1996) Structure of the sodium channel pore revealed by serial cysteine mutagenesis. *Proc Natl Acad Sci U S A* **93:**300-304

Pines G, Kanner BI (1990) Counterflow of L-glutamate in plasma membrane vesicles and reconstituted preparations from rat brain. *Biochemistry* **29:**11209-11214

Reyes N, Ginter C, Boudker O (2009) Transport mechanism of a bacterial homologue of glutamate transporters. *Nature* **462:**880-885

Shlaifer I, Kanner BI (2007) Conformationally sensitive reactivity to permeant sulfhydryl reagents of cysteine residues engineered into helical hairpin 1 of the glutamate transporter GLT-1. *Mol Pharmacol* **71:**1341-1348

Shrivastava IH, Jiang J, Amara SG, Bahar I (2008) Time-resolved mechanism of extracellular gate opening and substrate binding in a glutamate transporter. *J Biol Chem* **283:**28680-28690

Slotboom DJ, Sobczak I, Konings WN, Lolkema JS (1999) A conserved serine-rich stretch in the glutamate transporter family forms a substrate-sensitive reentrant loop. *Proc Natl Acad Sci U S A* **96:**14282-14287

Storck T, Schulte S, Hofmann K, Stoffel W (1992) Structure, expression, and functional analysis of a Na(+)-dependent glutamate/aspartate transporter from rat brain. *Proc Natl Acad Sci U S A* **89:**10955-10959

Tanaka K (1993) Expression cloning of a rat glutamate transporter. *Neurosci Res* **16:**49-153

Verdon G, Boudker O (2012) Crystal structure of an asymmetric trimer of a bacterial glutamate transporter homolog. *Nat Struct Mol Biol* **19:**355-357

Yernool D, Boudker O, Jin Y, Gouaux E (2004) Structure of a glutamate transporter

homologue from Pyrococcus horikoshii. *Nature* **431:**811-818

Zerangue N, Kavanaugh MP (1996) Flux coupling in a neuronal glutamate transporter. *Nature* **383:**634-637

Zhang Y, Zhang X, Qu S (2014) Cysteine mutagenesis reveals alternate proximity between transmembrane domain 2 and hairpin loop 1 of the glutamate transporter EAAT1. *Amino. acids.* **46:**1697-1705

Zomot E, Zhou Y, Kanner BI (2005) Proximity of transmembrane domains 1 and 3 of the gamma-aminobutyric acid transporter GAT-1 inferred from paired cysteine mutagenesis. *J Biol Chem* **280:**25512-25516

Molecular Pharmacology Fast Forward. Published on September 29, 2014 as DOI: 10.1124/mol.114.094995
This article has not been copyedited and formatted. The final version may differ from this version.

FOOTNOTES

This work was supported by the National Natural Science Foundation of China Grant [31170734], the International Centre for Genetic Engineering and Biotechnology Grant [CRP/CHN11-01], the Specialized Research Fund for the Doctoral Program of Higher Education Grant [20114433120002] and the Specialized Research Fund for talent introduction of colleges and universities of Guangdong Province Grant [2011430-1]. The authors declare no competing financial interests.

Molecular Pharmacology Fast Forward. Published on September 29, 2014 as DOI: 10.1124/mol.114.094995
This article has not been copyedited and formatted. The final version may differ from this version.

FIGURE LEGENDS

FIGURE 1. The outward- and inward-facing structures of Glt_{Ph}. The crystallized outward- (A) and inward-facing (B) forms of Glt_{Ph} are shown here (respective PDB codes 2NWW and 3KBC), aligned using the scaffold transmembrane (TM) helices 2, 4 and 5. Both structures are viewed from the same angle with the scaffold TM domains shown as cyliners (*gray, TM 2 and 5 transparent for clarity*) while the transport core domains TM7 (*orange*), TM8 (*purple*) and the two hairpin (HP) loops 1 and 2 (*yellow and red, respectively*) are shown as ribbons. (A) In the outward-facing form, proximity (*discontinuous black line*) between Val-151 (TM4) and Ser-279 (HP1) in Glt_{Ph} (*Cβ atoms shown as green and cyan spheres, respectively*), the equivalents of Ala-243 and Ser-366 in EAAT1, is shown while that in the inward-facing form (B) is shown for Val151/Met365 and Val151/Glu368, the respective equivalents of Ala243/Ile453 and Ala243/Thr456 pairs on TM4/HP2 in EAAT1. The extracellular loop between TM3 and 4 (*EL3-4*) shown here in (A) is superposed from the TBOA-bound outward-facing structure (PDB code 2NWW).

FIGURE 2. Effect of CuPh on the activity of single and double-cysteine mutants of EAAT1. (A) Dose-response effect of CuPh on D-[^{3}H]-aspartate transport activity of WT- and A243C/S366C-EAAT1. (B) Effect of 800 µM CuPh on activity of HeLa cells expressing WT, A243C/S366C or the indicated single-cysteine or control mutants, or those cotransfected with both single cysteine mutants (*A243C co S366C*). In each case, cells were treated with CuPh in NaCl solution for 5 min before the transport assay. Data represent percentage of the remaining uptake activity of samples relative to those without any treatment (mean ± S.E., n=3). Values different from that of EAAT1 with one-way ANOVA results of $p < 0.05$ or < 0.01 are indicated with one or two asterisks, respectively.

FIGURE 3. Inhibition of transport of cysteine mutants by cadmium. HeLa cells expressing A243C/S366C or the indicated mutants were washed once with choline chloride-containing solution and assayed for transport in the presence or absence of 500 µM cadmium chloride. Values shown are the percentage activity in the presence of 500 µM cadmium chloride relative to that in its absence. Values represent the mean ± S.E. of at least

Molecular Pharmacology Fast Forward. Published on September 29, 2014 as DOI: 10.1124/mol.114.094995
This article has not been copyedited and formatted. The final version may differ from this version.

three different experiments done in triplicates. Values different from that of EAAT1 with one-way ANOVA results of $p < 0.05$ or < 0.01 are indicated with one or two asterisks, respectively.

FIGURE 4. Effect of the composition of the external medium on inhibition by CuPh or MTSET. (A) HeLa cells expressing A243C/S366C were preincubated for 5 min in the presence and absence of 200 µM CuPh. The indicated preincubation solutions contained NaCl, NaCl + 1 mM L-glutamate, choline chloride (ChCl) + 1 mM L-glutamate, NaCl + 1 mM GABA, NaCl + 20 µM TBOA, ChCl + 20 µM TBOA, KCl or ChCl. (B) A243C- expressing HeLa cells were preincubated for 5 min in the presence or absence of 2.0 mM MTSET in the indicated solution before the transport assay. Values are given as percent of control (preincubation without CuPh or MTSET) and represent the mean ± S.E. of at least three different experiments done in triplicates. Values different from that in NaCl with one-way ANOVA results of $p < 0.05$ or < 0.01 are indicated with one or two asterisks, respectively.

FIGURE 5. Inhibition of A243C/I453C and A243C/T456C by CuPh or cadmium. (A) Dose-response of inhibition of uptake activity by CuPh in NaCl for A243C/I453C (*squares, continuous line*) or A243C/T456C (*circles, discontinuous line*)in CL-EAAT1. Inhibition of transport by 15 µM CuPh (B, C) or 500 µM Cd^{2+} (D, E) in NaCl solution is shown for the indicated constructs in CL-EAAT1 background. Values are given as percent of control (preincubation without CuPh or Cd^{2+}) and represent the mean ± S.E. of at least three different experiments done in triplicates. Values different from that of CL-EAAT1 with one-way ANOVA results of $p < 0.05$ or < 0.01 are indicated with one or two asterisks, respectively.

FIGURE 6. Effect of the composition of the external solution on the aqueous accessibility of I453C or T456C, and on the proximity of each site to A243C. (A, B) Shown here is the inhibition of activity in A243C/I453C (A) or A243C/T456C (B) by 5 µM CuPh under various external conditions as indicated. The aqueous accessibility of cysteine inserted at each position, in I453C (C) or T456C (D), is shown as a function of the impact on activity in each construct by 0.05 (C) or 2.0 (D) mM MTSET under the indicated external

Molecular Pharmacology Fast Forward. Published on September 29, 2014 as DOI: 10.1124/mol.114.094995
This article has not been copyedited and formatted. The final version may differ from this version.

conditions. Values are given as percent of control (preincubation without CuPh or MTSET) and represent the mean ± S.E. of at least three different experiments done in triplicates. Values different from those in NaCl with one-way ANOVA results of $p < 0.05$ or < 0.01 are indicated with one or two asterisks, respectively.

Molecular Pharmacology Fast Forward. Published on September 29, 2014 as DOI: 10.1124/mol.114.094995
This article has not been copyedited and formatted. The final version may differ from this version.

TABLES

Table 1. Kinetic parameters of transporter mutants in the absence or presence of CuPh. V_{max} and K_m values were calculated for each mutant in the absence or presence of CuPh. V_{max} is shown as a percentage of EAAT1 or CL-EAAT1 without CuPh treatment while K_m is shown in μM. Mutants in the upper part of the table are in the background of EAAT1, others in the lower part of the table are in the background of CL-EAAT1. Values are expressed as mean ± S.E for at least three times independent repeated experiments. Statistical analysis results different from the control (without treatment of CuPh) are expressed as $p < 0.05$ or < 0.01 with one or two asterisks respectively by using Student's *t* test.

	V_{max}	K_m	**800μM CuPh**	
			V_{max}	K_m
EAAT1	100	28.7±3.5	92.6±5.2	30.6±2.8
A243C/S366C	36.2±4.8	39.2±6.3	20.1±2.2 *	42.3±3.8
A243C	80.2±4.2	37.2±4.4	81.3±3.6	39.8±3.5
S366C	40.3±5.1	36.3±4.2	45.1±3.9	38.5±2.6
	V_{max}	K_m	**15μM CuPh**	
			V_{max}	K_m
CL-EAAT1	100	30.6±1.2	93.2±2.9	28.4±3.3
A243C/I453C	82.7±1.9	26.0±1.4	52.7±3.6 * *	52.6±8.4 *
A243C/T456C	62.6±1.1	35.9±3.4	35.7±4.5 * *	45.1±2.1
A243C	86.7±3.2	35.8±3.5	87.5±2.4	40.1±4.7
I453C	55.2±4.7	31.4±4.4	57.4±3.4	32.3±4.1
T456C	38.9±3.6	29.5±4.1	38.2±4.3	30.3±3.9

Figure 1

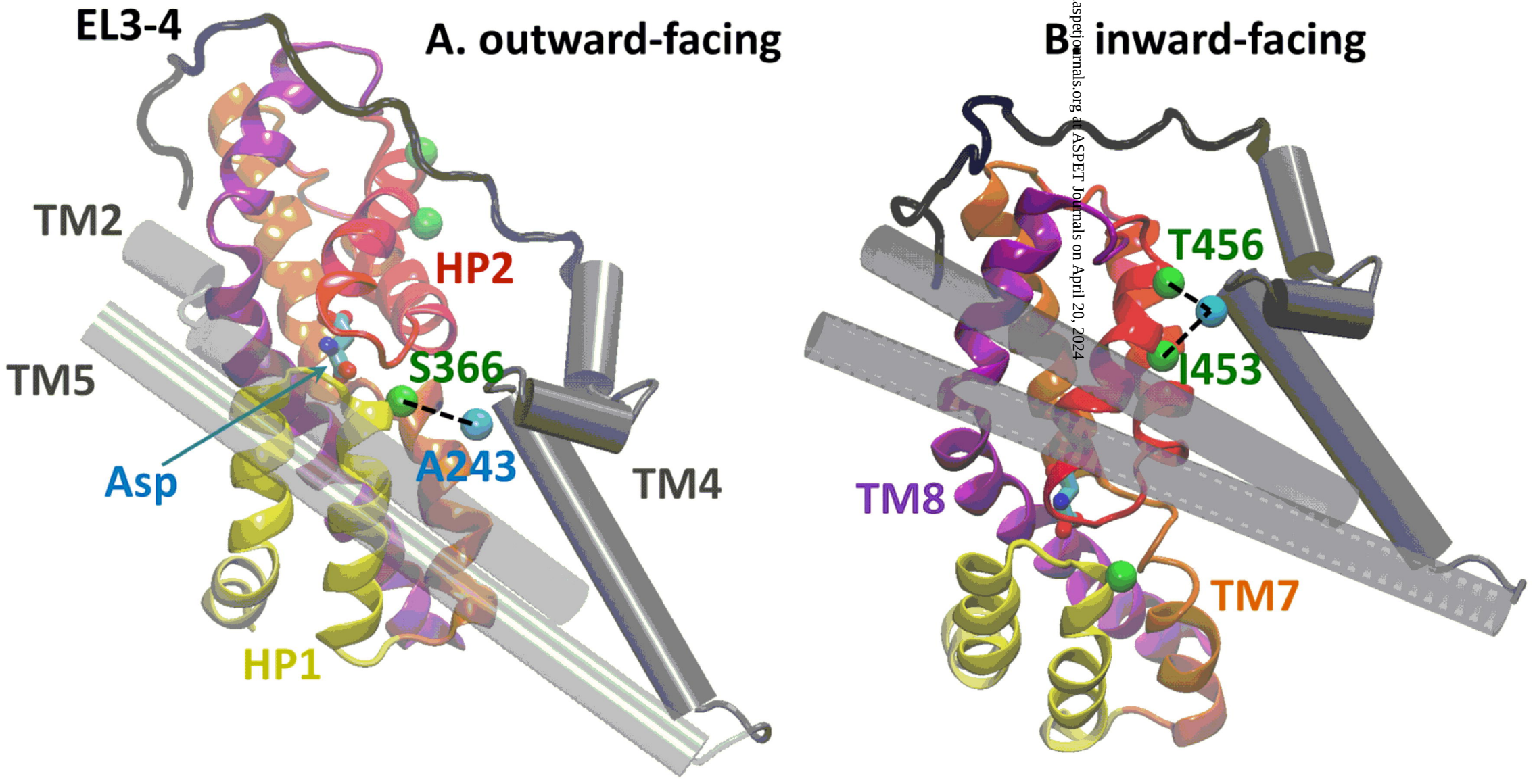

Figure 2

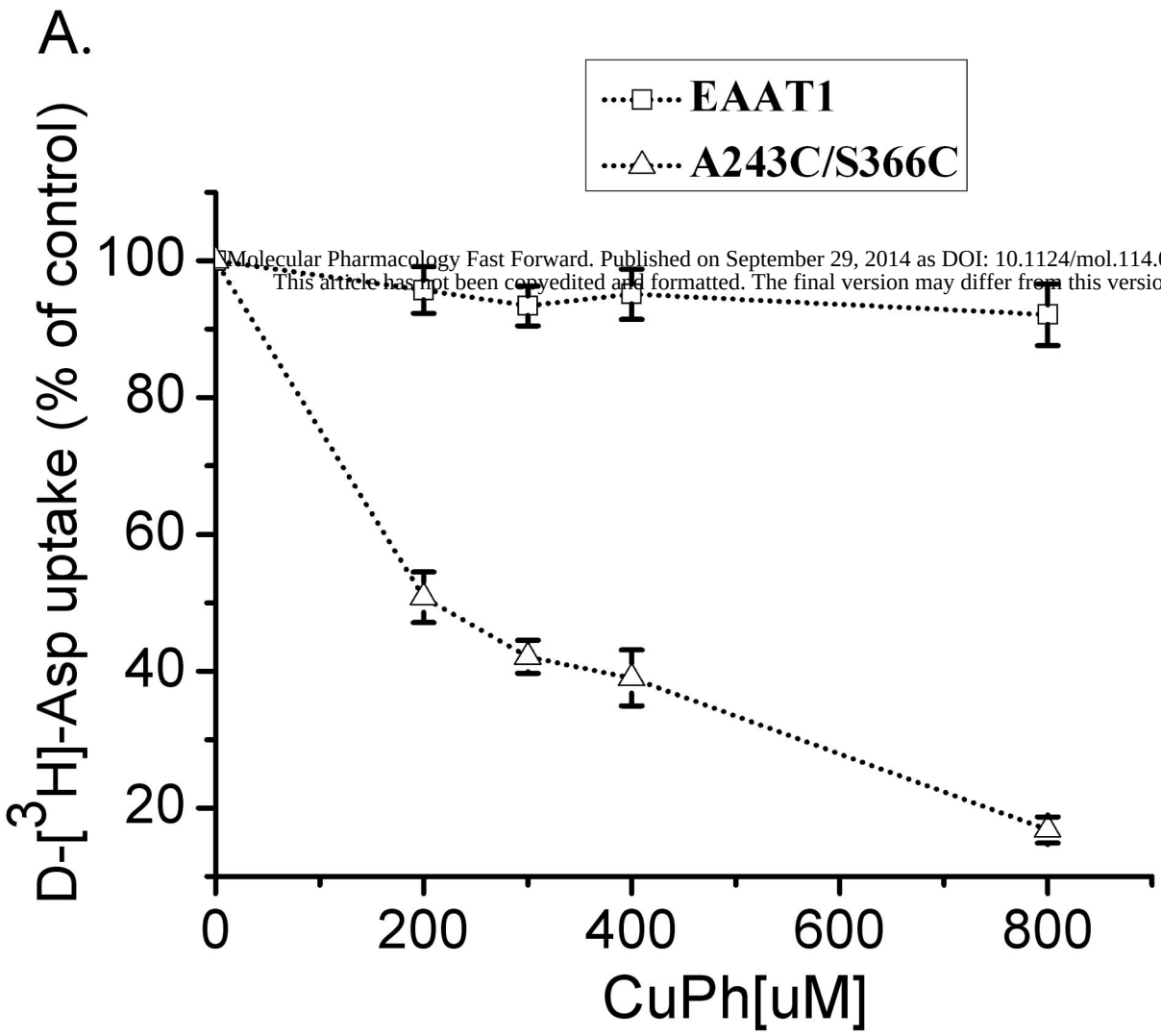

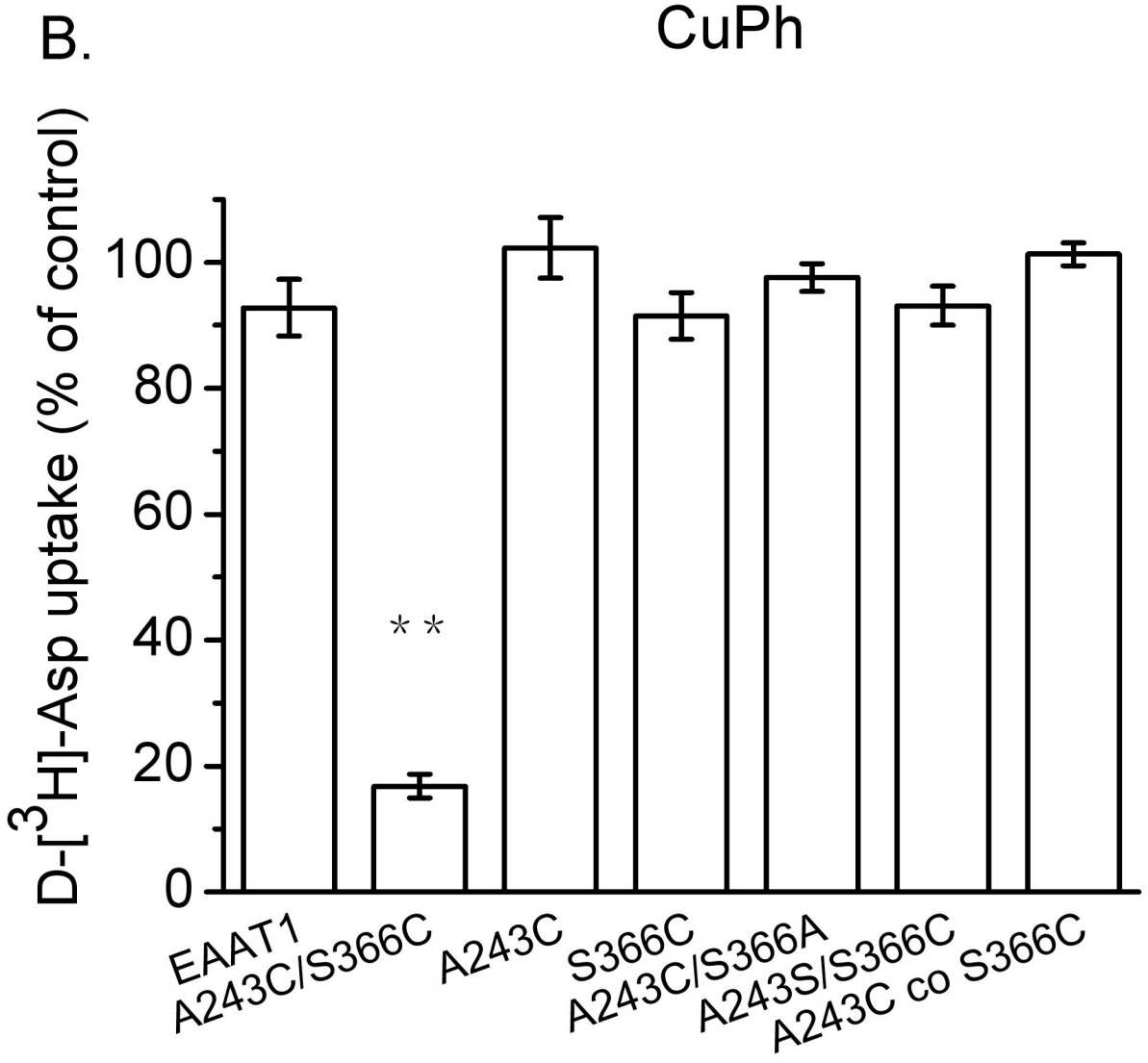

Figure 3

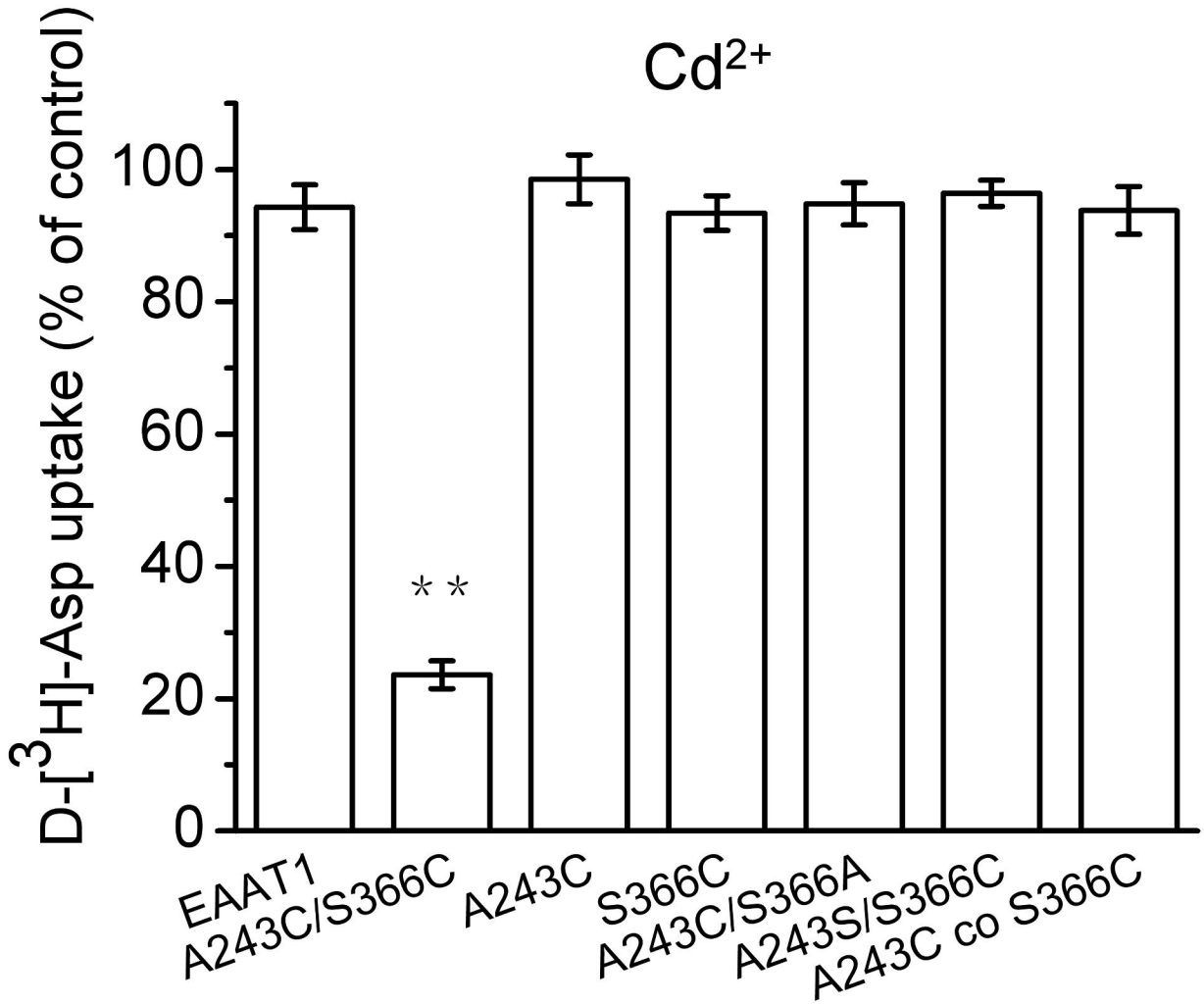
Cd2+
D-[3H]-Asp uptake (% of control)
100
80
60
40
20
0
* *
EAAT1
A243C/S366C
A243C
S366C
A243C/S366A
A243S/S366C
A243C co S366C

Figure 4

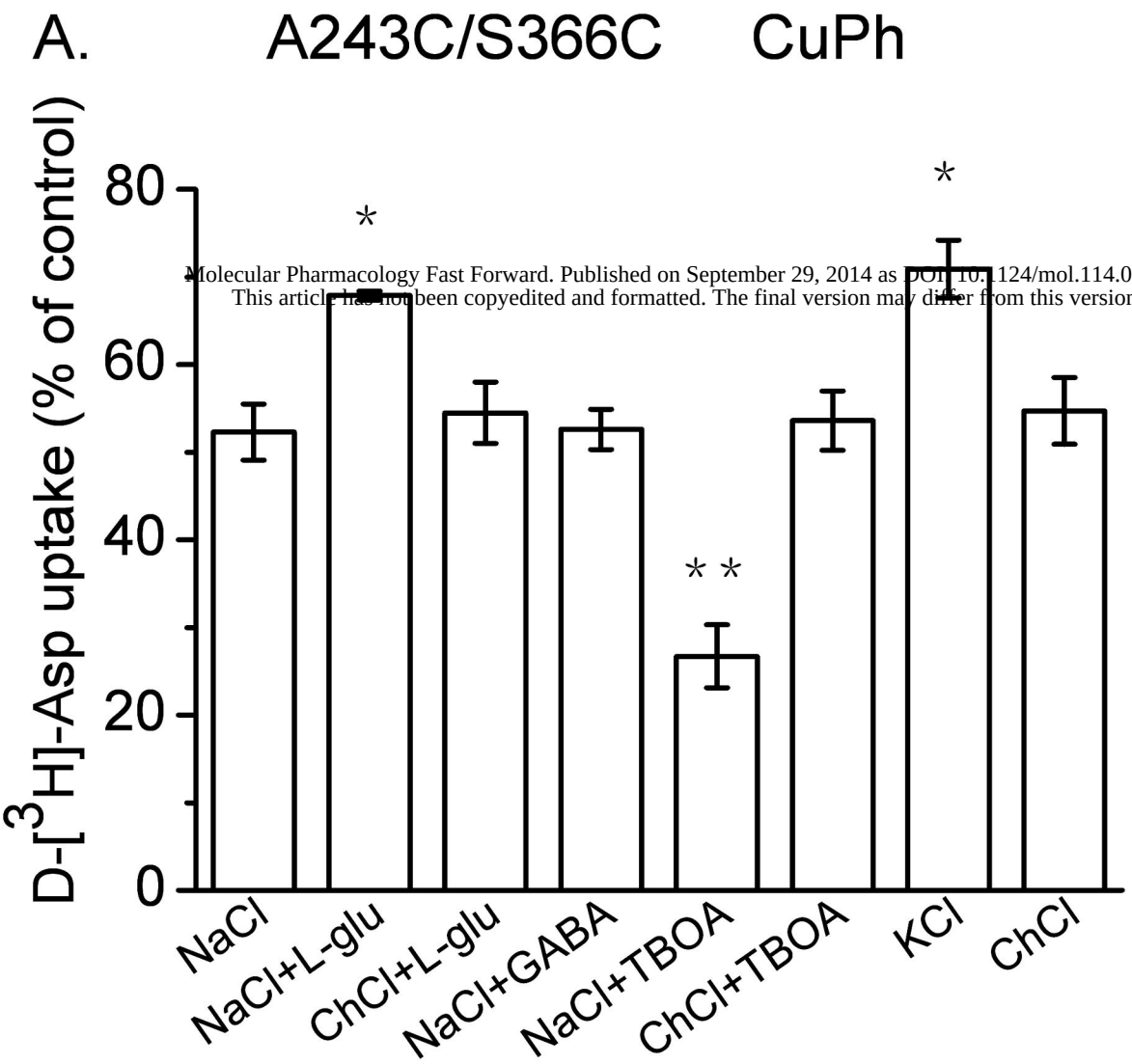

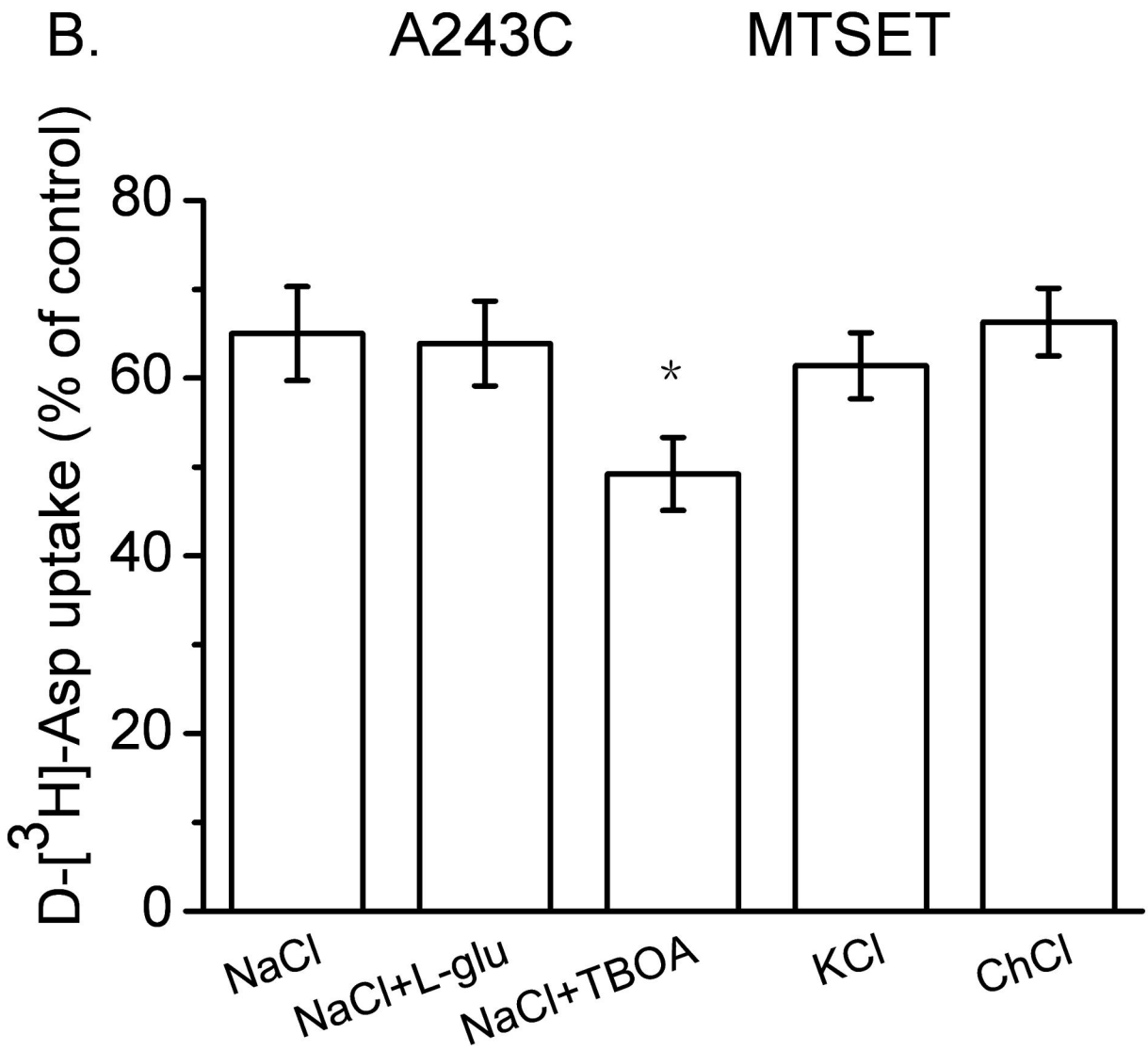

Figure 5

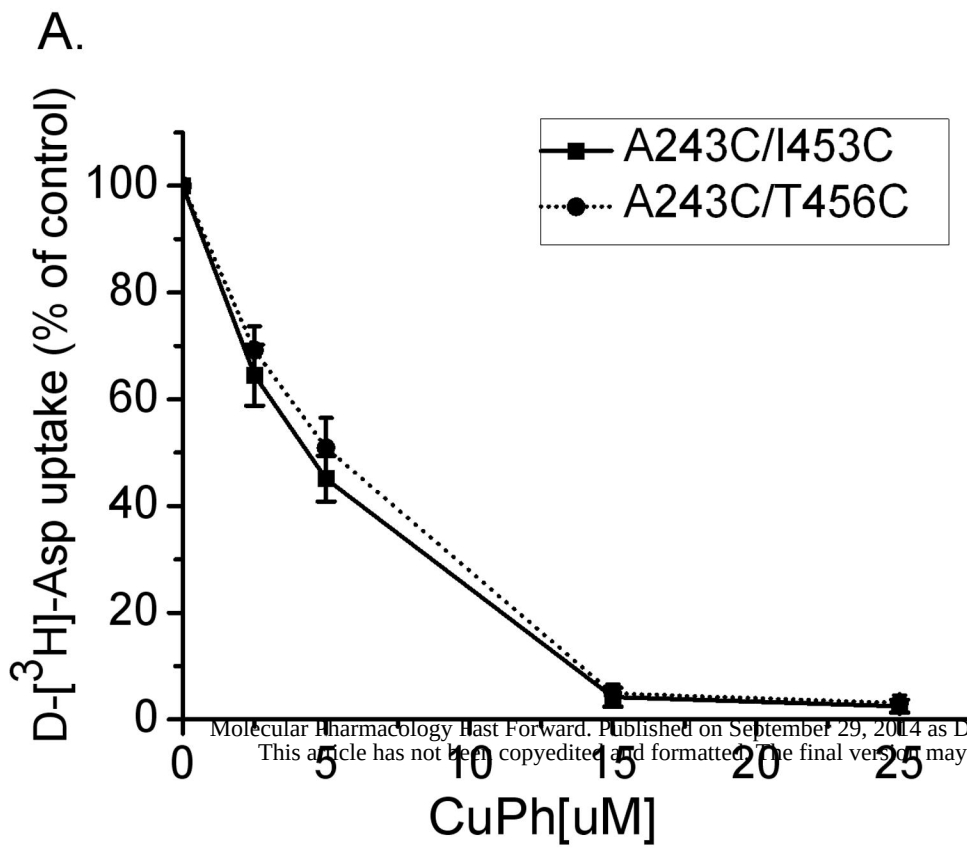

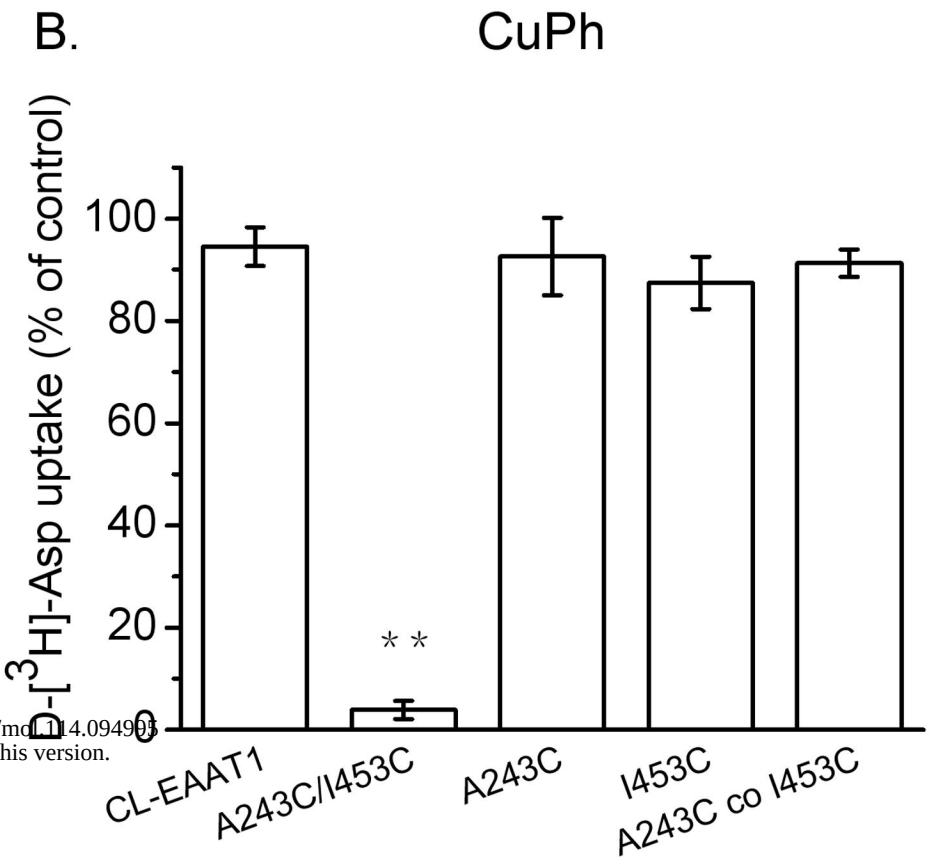

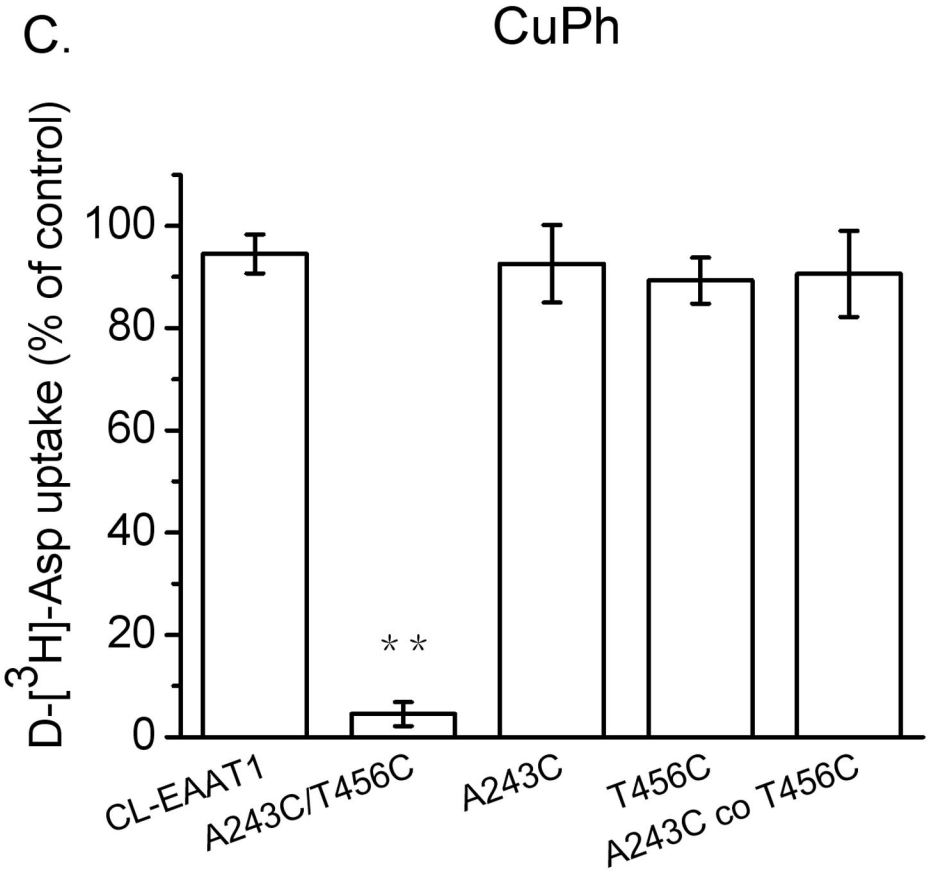

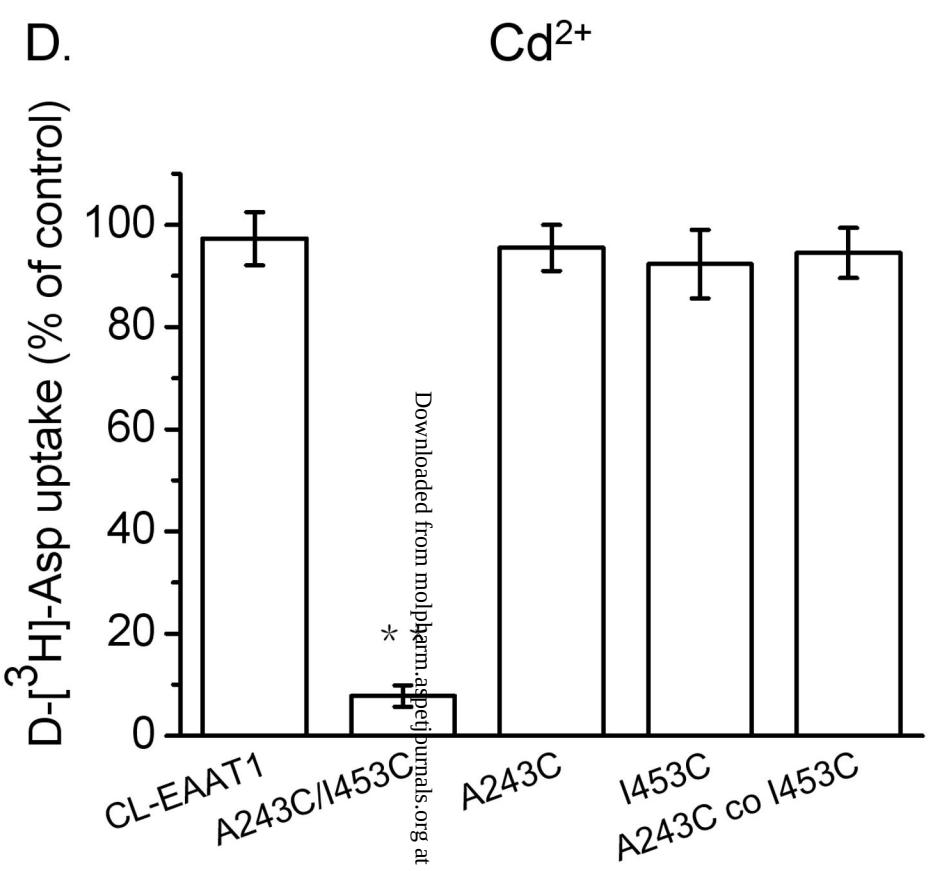

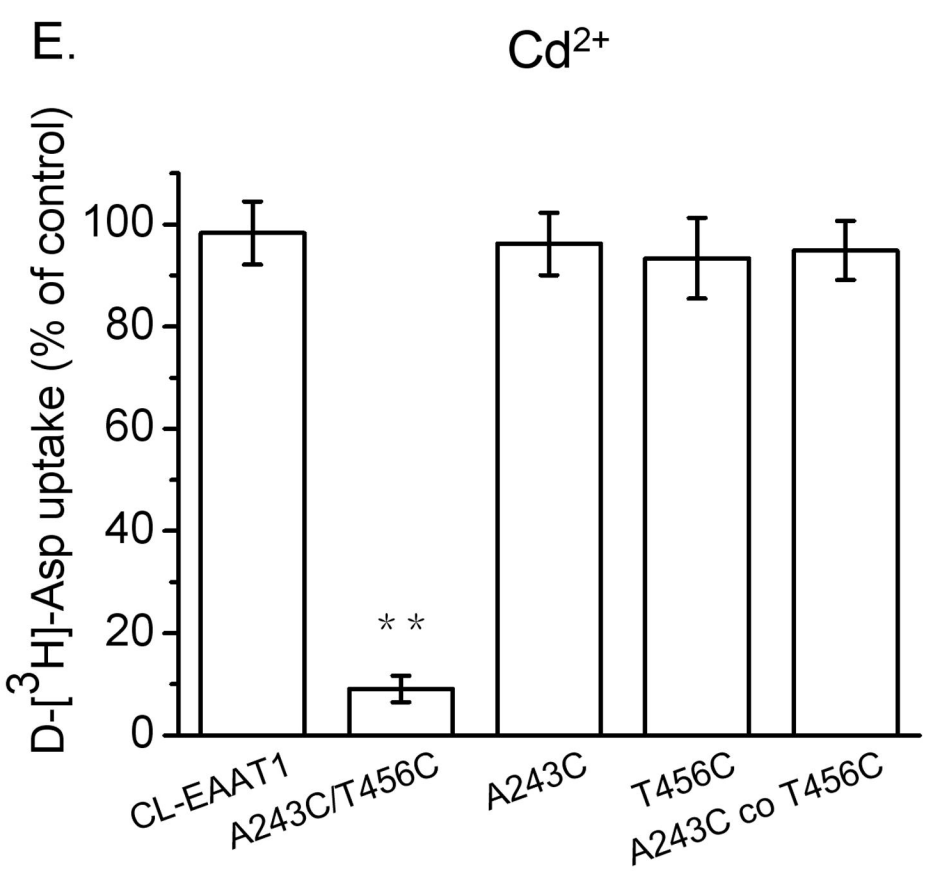

Figure 6